International Journal of Minerals, Metallurgy and Materials
Volume 22, Number 3, March 2015, Page 309
DOI: 10.1007/s12613-015-1075-1

Investigation on the interface of Cu/Al couples during isothermal heating

Yan-qiu Han, Li-hua Ben, Jin-jin Yao, Shu-wei Feng, and Chun-jing Wu

School of Materials Science and Engineering, University of Science and Technology Beijing, Beijing 100083, China

(Received: 16 June 2014; revised: 9 October 2014; accepted: 11 October 2014)

Abstract: The evolutionary process and intermetallic compounds of Cu/Al couples during isothermal heating at a constant bonding temperature of 550°C were investigated in this paper. The interfacial morphologies and microstructures were examined by optical microscopy, scanning electron microscopy equipped with energy dispersive X-ray spectroscopy, and X-ray diffraction. The results suggest that bonding is not achieved between Cu and Al at 550°C in 10 min due to undamaged oxide films. Upon increasing the bonding time from 15 to 25 min, however, metallurgical bonding is obtained in these samples, and the thickness of the reactive zone varies with holding time. In the interfacial region, the final microstructure consists of Cu_9Al_4, CuAl, $CuAl_2$, and α-Al + $CuAl_2$. Furthermore, these results provide new insights into the mechanism of the interfacial reaction between Cu and Al. Microhardness measurements show that the chemical composition exerts a significant influence on the mechanical properties of Cu/Al couples.

Keywords: copper; aluminum; intermetallic compounds; oxide films; isothermal heating

1. Introduction

Laminated composites are becoming increasingly important in industrial applications due to their numerous advantages. In many cases, through the choices of laminated architecture, component materials, and processing history, laminated systems can be devised to produce a material with prescribed properties [1]. Systems based on Cu and Al are typically identified as candidate materials for electric devices such as transition pieces in high direct-current bus systems [2] or conductive strips used in high frequency alternative current equipment [3]. Recently, some studies have been performed on the Cu/Al system to investigate mechanical properties [4–5] and diffusion behavior [6–7]. Heness *et al*. [4] investigated the interfacial strength evolution of roll-bonded Cu/Al laminates and showed that the phases generated in the interfacial region dominated the interfacial strength. Guo *et al*. [7] studied intermetallic phase formation in diffusion-bonded Cu/Al laminates prepared by plasma-activated sintering in the temperature range of 400–500°C. They reported that $CuAl_2$ was the first phase among three intermetallic phases ($CuAl_2$, CuAl, Cu_9Al_4) on the basis of the effective heat of formation model. Meanwhile, several processing techniques such as roll bonding [8], friction welding [9], and reactive diffusion bonding [10] have been used to fabricate Cu/Al laminated composites. All of these methods are solid state techniques that are performed below the eutectic temperature (548.2°C). Investigations of the solid state bonding of metals [3–5,8] have demonstrated that with the combination of pressure and heat, the reactive mechanism between metals is as follows: (1) development of physical contact; (2) activation of the surfaces in contact; and (3) interactions within the materials being joined. It should be noted that Kawakami *et al.* [11] studied Cu/Al dissimilar bonding in a temperature range above the eutectic temperature and below the melting point of aluminum. They pointed out that in such dissimilar bonding, diffusion started from the adherence surface of both metals after the breaking of the oxide films. Furthermore, the thickness increase of the oxide film was suppressed by the reduction in the oxygen concentration in the atmosphere surrounding the bond area. However, the evolutionary process of intermetallic phase formation at the Cu/Al interface remains uncertain.

This study focuses on the intermetallic phase formation at the Cu/Al interface during isothermal heating at 550°C for

Corresponding author: Chun-jing Wu E-mail: cjwu@mater.ustb.edu.cn

different holding times. The interfacial morphology and hardness of the couples are examined. The sequence of phase formation is rationalized, and the related mechanism is discussed based on the experimental observations.

2. Experimental

Commercially available Cu (99.9%) and Al (99.6%) rods with a diameter of 10 mm were cut into specimens with a length of 8 mm. The specimen surfaces for bonding were mechanically ground on 400–2000 emery papers. It is extremely important to clean the samples prior to the bonding process in order to minimize the occurrence of voids/defects within the resulting couples. For this reason, all surfaces were degreased in acetone to remove adhered contaminants and dried in air before the experiments. Subsequently, the Cu and Al samples were immersed in 10vol% H_2SO_4 and 10vol% NaOH solution, respectively, to remove oxides on the surfaces. The Al specimens also had to be deactivated in 10vol% HNO_3 solution. Finally, all the samples were rinsed with ethanol and then stored in ethanol until the bonding trial.

After the surface treatment, the samples were stacked in the furnace with the upper one being copper and the lower one being aluminum. They were then processed by a specially designed bonding apparatus, which is shown schematically in Fig. 1. The oxide film is known to form very rapidly on the surface of the aluminum or copper, thus, it acts as a barrier to the formation of a metallurgical bond [12]. Therefore, the time interval between surface preparation and experiment was kept to less than 2 min to avoid the formation of thick and continuous oxide layers on the sample surfaces [2]. The experiment was conducted under a uniaxial pressure of 0.3 MPa in argon atmosphere, which was introduced at a rate of 400 L/h, to further limit oxidation. A heating rate of 40°C/min was used to bring the couples to a temperature of 550°C for different durations (10, 15, 20, and 25 min) followed by air cooling. To accurately measure the temperature, a K-type thermocouple was inserted into the copper cylinder near the interface. In view of the evolution of the interfacial structures, experiments were carried out at a relatively low bonding temperature (550°C) that was above the eutectic temperature (T_E = 548.2°C) of the Cu/Al system to avoid the significant deformation that occurs at higher temperatures as well as the excessive formation of Cu–Al intermetallic compounds (IMCs) [11]. Vertical pressure was applied to the bonding couples to attain intimate contact between Cu and Al and then to obtain liquid phase by contact reaction in order to remove the voids in the bonding interface [13]. For metallographic examination, bonded samples were cut transversely through the couples, and the surfaces were polished to a 0.5 μm finish using a diamond suspension. The macrostructures of the couples were examined by optical microscopy. Scanning electron microscopy (SEM) equipped with energy dispersive spectroscopy (EDS) was used to examine the microstructure and determine the phases in the interfacial region. In order to study the morphology of IMCs at the interface, the specimens were etched with 10vol% HF solution for about 3–5 s after grinding and polishing. The brittle interface surface was analyzed by X-ray diffraction (XRD) using the diffractometer technique. To determine the Vickers hardness across the bonded interface, hardness testing was carried out at a load of 50 g for a testing time of 10 s.

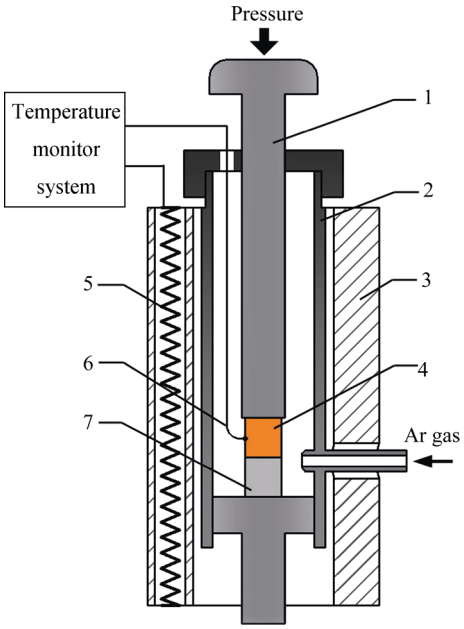

Fig. 1. Schematic of the apparatus used for isothermal bonding: 1—pressure plunger; 2—furnace lining; 3—furnace; 4—copper; 5—resistance wire; 6—thermal couple; 7—aluminum.

3. Results and discussion

3.1. Effect of bonding time on the reactive zone

At first, diffusion occurs in the limited contact points of the Cu–Al surface [8] due to the combination of the bonding temperature and the uniaxial pressure. According to the Cu–Al binary phase diagram, there exists a eutectic reaction at 548.2°C with the composition of 66.8wt% Cu and 33.2wt% Al. Once the temperature reaches 550°C, the contact reaction is triggered to form liquid at the Cu/Al interface. With the nucleation of eutectic liquid at the limited points, both Cu and Al atoms quickly diffuse into the liquid since

diffusion is about 100–1000 times faster in liquid than in solid [14]. Thus, the liquid continues to be produced, and the contact points also increase. As the curvature of the liquid at the contact parts increases, the produced liquid moves along the surface, indicating that the surface tension has increased [15]. As time elapses, metallurgical bonding can be anticipated due to the significant interdiffusion and contact reaction. Nevertheless, bonding is not achieved at a holding time of 10 min (Fig. 2). This might be explained by the fact that the liquid is not sufficient to produce a sound bond in a holding time of 10 min. Fig. 3 shows the XRD pattern of the uncombined couple performed at 550°C for 10 min. During isothermal heating, the reactions between Cu and Al can be described by the following equations:

$$\text{Cu (s)} + \text{Al (s)} \rightarrow \text{(Cu, Al) (l)} \quad (1)$$

$$\text{(Cu, Al) (l)} \rightarrow \text{CuAl}_2\text{ (s)} + \alpha\text{-Al (s)} \quad (2)$$

where s and l indicate that the reactant is in the solid and liquid phase, respectively. In the diffraction patterns of the sample, only Al_2O_3 is detected on the aluminum side (Fig. 3(a)). Only a small fraction of Al phase exists on the copper side, as reflected by its low intensity peaks (Fig. 3(b)). Hence it is Al_2O_3 rather than the Cu oxide film that hinders the contact reaction, and the amount of $CuAl_2$ might be too small to be detected. In addition, the significant difference in the thermal expansion between Cu (9.4×10^{-6}/°C) and Al (23.6×10^{-6}/°C) during heating results in the uncombined sample as well as the bond stress in the cooling process from 550°C to ambient temperature [5].

Fig. 2. Appearance of an uncombined Cu/Al couple bonded at a temperature of 550°C for 10 min.

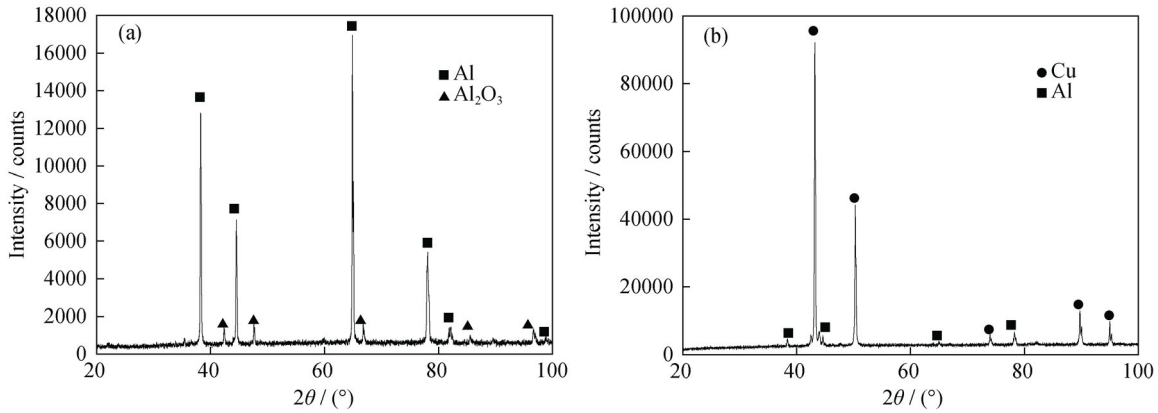

Fig. 3. X-ray diffraction patterns measured on the uncombined couple processed at 550°C for 10 min: (a) Al side; (b) Cu side.

Fig. 4 shows the typical appearances and corresponding cross-sectional macrostructures of the bonded Cu/Al couples fabricated at 550°C for 15, 20, and 25 min. Such results can be expected based on two factors. First, the formation of IMCs is dependent on the bonding time because Cu and Al atoms are thermally activated [4]. Second, with longer holding time, the breakage of the oxide films is more significant, thus providing virgin surfaces. A longer holding time also creates more contact area between the asperities to enhance diffusion bonding. The extruded liquid phase is observed on the surface of each sample (Figs. 4(a), 4(c), and 4(e)), and the three bonded samples show relatively smooth surfaces. In Figs. 4(b), 4(d), and 4(f), the cross-sections of the Cu/Al couples formed at various bonding times can be observed, and the Cu/intermetallic zones and intermetallic zone/Al interfaces are flat and clearly distinguishable. The initial interface and a number of interfacial voids between faying surfaces are clearly observed, as shown in Figs. 4(b), 4(d), and 4(f). This could be a consequence of the rough macroscopic surfaces of the as-bonded copper and aluminum, leading to the presence of voids that are very difficult to suppress afterwards [16]. The sizes and shapes of the voids depend on the initial roughnesses of the bonding surfaces. However, in the present case, the voids are not very significant and, no cracks are observed in the intermetallic zone. This might be attributed to the integrated effect of higher temperature compared to solid-state bonding technology and pressure application in this study. Wu *et al*. [17] confirmed that increasing bonding temperature or pressure resulted in a significant decrease in the time required for the elimination of voids.

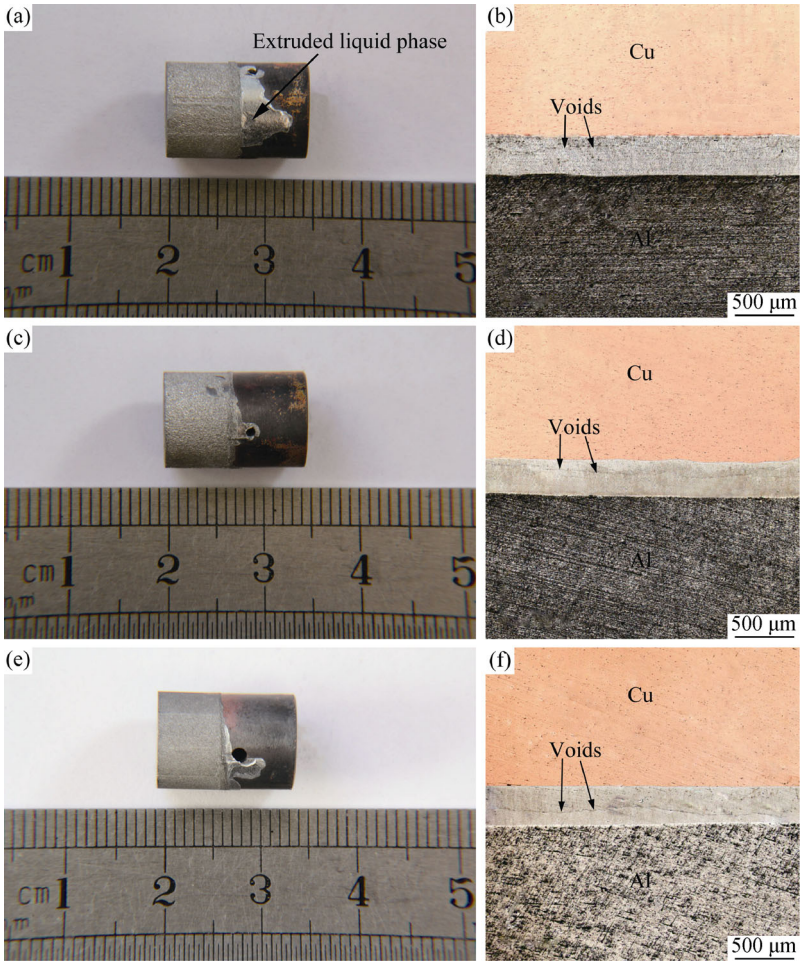

Fig. 4. Typical appearances and corresponding macrostructures of Cu/Al couples produced at 550°C for various time: (a) and (b) 15 min; (c) and (d) 20 min; (e) and (f) 25 min.

From the cross-sectional optical images (Fig. 4(b)), the thickness L of the intermetallic zone is evaluated by the equation:

$$L = A/W \quad (3)$$

where W and A are the total length parallel to the initial Cu/Al interface and the total area of the intermetallic zone, respectively, on the cross-section. The results for the samples with bonding durations of 15, 20, and 25 min are presented in Table 1. Thus, the thickness of the reactive zone (L_2) is reliably determined by the equation:

$$L_2 = L_0 - L_1 + L. \quad (4)$$

where L_0 is the total thickness of the copper and aluminum cylinder after grinding and L_1 is the thickness of the bonded Cu/Al couple. This indicates that the reactive zone is made up of the extruded liquid phase and the intermetallic zone. From the experimental values in Table 1, it can be concluded that the thickness of the reactive zone increases from 1227 μm to 1423 μm as the holding time increases from 15 to 25 min. The large thickness value of the IMCs in this study is consistent with the magnitude of bonding fabricated by horizontal core-filling continuous casting technology [18] but much larger than those processed by solid-state bonding methods at lower temperatures [3,19–21].

Table 1. Thickness values obtained at different holding times

Time / min	L_0 / mm	L_1 / mm	L / μm	L_2 / μm
15	15.767	14.852	312	1227
20	15.821	14.817	297	1301
25	15.577	14.470	316	1423

3.2. Microstructure

3.2.1. Interfacial microstructure

SEM micrographs of the Cu/Al couple produced at 550°C for 20 min are shown in Fig. 5. All the micrographs were taken in the back-scattered electron mode. Different phases were identified, and the EDS analysis results are listed in Table 2. Fig. 5(a) shows an overview of SEM morphology at the intermetallic zone of the Cu/Al couple. A higher magnification image of region I (Fig. 5(b)) shows that some structures (P3–P5) are generated between copper

(P1, P2) and the eutectic (P6) structure. The EDS analysis results (Table 2) identify these structures (P3, P4, and P5) as Cu_9Al_4, CuAl, and $CuAl_2$, respectively. The phases formed here are consistent with those found in the interfacial zone of the Cu/Al couple in compound casting [22]. Region II is exactly a part of the eutectic zone, and Fig. 5(c) shows a higher magnification image. It contains two types of eutectic zones (α-Al+$CuAl_2$), the anomalous one (P7) and the lamellar one (P8). Unlike region I, in which some different phases could be distinguished, Al only exists as an Al-based solid solution α-Al (P10) between aluminum (P11) and the eutectic (P9) structure in region III (Fig. 5(d)).

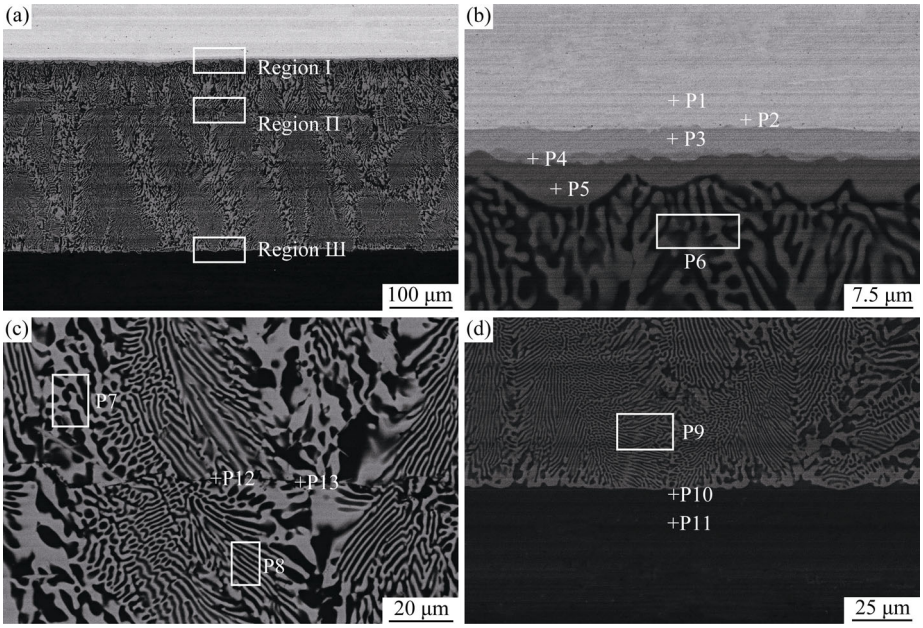

Fig. 5. Interfacial microstructures of Cu/Al couples produced at 550°C for 20 min: (a) cross-sectional overview; (b–d) magnified views of regions I–III marked in (a).

Table 2. EDS analysis results of the sample bonded at 550°C for 20 min

Positions	Region	Al / at%	Cu / at%	O / at%
P1	I	0	100	0
P2	I	0	100	0
P3	I	34.59	65.41	0
P4	I	50.57	49.43	0
P5	I	68.68	31.32	0
P6	I	79.84	20.16	0
P7	II	85.03	14.97	0
P8	II	80.09	19.91	0
P9	III	73.32	26.68	0
P10	III	96.63	3.37	0
P11	III	100	0	0
P12	II	65.93	8.92	25.15
P13	II	71.46	25.48	3.05

3.2.2. Morphology and types of intermetallic compounds

Regardless of holding time, three phases were observed between copper and the eutectic zone in all experiments. A scallop-shaped $CuAl_2$ layer appears at the interface between copper and the eutectic zone, as shown in Fig. 5(b). This morphology is in good agreement with the Young–Laplace equation [23] and has been observed in previous experiments [18,24–25]. Once the $CuAl_2$ layer has formed, a grooved-type morphology begins to develop at the $CuAl_2$/$CuAl_2$ and $CuAl_2$/eutectic phase grain boundary (GB) triple junctions. This scallop-shaped morphology is caused by the faster mass transport across the GBs than in the bulk phase [26]. It should be noted that the Cu_9Al_4 layer is thin, and its thickness is almost uniform. A reasonable explanation for this is that Cu_9Al_4 is generated through the solid-state phase transformation from $CuAl_2$ to Cu_9Al_4 since the diffusion coefficient of the atom in the solid is much smaller than that in the liquid, and the diffusion time is insufficient. Meanwhile, it makes sense to assume that all of the CuAl is formed during cooling because the CuAl layer is isolated at the $CuAl_2$/Cu_9Al_4 interface.

In Fig. 5(c), the anomalous region has well-defined α-Al dendrite cells, and α-Al is surrounded by a ribbon-like $CuAl_2$ phase (gray). The lamellar eutectic region has lamellae of α-Al and $CuAl_2$. Due to a relatively higher interfacial energy in the fine lamellar eutectic structure, the reduction

of this energy will act as a driving force for the transformation of the fine lamellar eutectic to a coarser microstructure of anomalous eutectics, which are thermodynamically more stable. In the present study, the α-Al dendrite phase solidified first and released heat to the interdendritic molten phase. Subsequently, this remnant melted, resulting in slight undercooling and solidification with a smaller growth velocity. Thus, the nucleation and growth rates of the two phases are distinct in the eutectic. This eventually gives rise to a large interlamellar distance, resulting in an anomalous structure [27].

3.3. Surface oxide films

The thicknesses and the corresponding times required for the formation of copper and aluminum oxide films are listed in Table 3 [22]. Despite the careful preparation of both copper and aluminum, oxide films may have formed rapidly at the interface. If the oxide films are not removed before contact between the metals, bonding will be affected to some extent. Fig. 3(a) illustrates that the existence of Al_2O_3 hinders the formation of an intimate contact between copper and aluminum. Thus, it is reasonable to take the removal of the oxide film from the interface as the beginning stage of the formation of IMCs at the interface [16]. In comparison with copper, aluminum has a higher tendency to oxidize due to its large free energy of oxide formation. Theoretically, the formed Al_2O_3 film can be thicker than the Cu oxide film. In fact, although the formation of aluminum oxide on the Al surface is rapid, it exhibits self-protection and is usually very thin. Additionally, the oxidation process of copper is kinetically faster than that of aluminum due to the porous structure of copper oxide film. Thus, the formed Cu oxide film is thicker than the Al_2O_3 film. Table 3 demonstrates that within 15 s, the thickness of the aluminum oxide film is 12×10^{-4} μm, whereas that of the copper oxide film is 15×10^{-4} μm. During isothermal heating, plastic deformation takes place in the contact points between micro-asperities, increasing the contact area. With increasing bonding time, there are more contact points. The eutectic liquid is first produced at some limited points and then spreads along the faying surfaces. Meanwhile, the bonded area is less than 100%, and many voids remain in the interface. Because of the small thickness of the eutectic liquid in the initial stage, the effect of convection in the liquid is assumed to be negligible. Owing to the uniaxial pressure, the two oxide films and the liquid are subjected to deformation forces, i.e., shear stress. The copper oxide film does not have enough strength and continuity to withstand the shear stress [28–29]. Since the oxide film has little or no plasticity, it will tear when subjected to shear stress [12]. Alumina oxide is also brittle and easily broken under external force. Structural defects in alumina oxide also weaken it, and the Al_2O_3 film is not strong enough to withstand the shear stress [30]. As a consequence, the oxide films tear to shreds that are removed with the extruded eutectic liquid, leaving the surfaces in contact. In other words, the fragments of oxide films are constantly diluted until no evident oxide film is found at the interface in Fig. 5. In this work, a proper bonding condition is attained with residual fragments of oxide films at the interface (P12, P13). Furthermore, owing to the protection of the surrounding atmosphere, clear oxide films are not observed in the entire intermetallic zone (Fig. 5), which can be ascribed to the reduction in the oxygen concentration.

Table 3. Oxide film thickness and time required for formation [22]

Metal	Film thickness / μm	Time / s	Equation
Copper	15×10^{-4}	15	$2Cu\ (s) + 1/2O_2\ (g) = Cu_2O\ (s)$
Aluminum	12×10^{-4}	15	$4/3Al\ (s) + O_2\ (g) = 2/3Al_2O_3\ (s)$

3.4. Evolutionary process and mechanism of interfacial reaction between Cu and Al

The fact that bonding is not achieved at 550°C for 10 min supports the notion that the removal of the oxide film from the interface is the beginning stage of the formation of IMCs at the interface between copper and aluminum. In contrast to the copper oxide film, the Al_2O_3 film is more difficult to remove to achieve diffusion bonding. The persistent oxide attached to the Al surface makes bonding difficult, as illustrated in Fig. 2. Compared with the copper side, no eutectic phase is detected at the aluminum side.

After the breaking of oxide films at some limited contact points, virgin metals extrude through the cracks and contact due to the uniaxial pressure [8]. Subsequently, interdiffusion begins with two atoms in this case. By increasing the holding time in the contact area, the concentration of copper atoms at the aluminum side near the interface reaches $C^{\alpha L}$ ($C^{\alpha L}$ is the chemical composition of the surface of aluminum adjacent to the liquid), resulting in the formation of α-Al based on Cu–Al phase diagram shown in Fig. 6. The diffusion coefficient of Cu in Al is higher than that of Al in Cu. This difference becomes more remarkable with increasing temperature [31]. It is possible to neglect the phase generated on the copper side at this stage as the volume of the area is considered to be extremely small compared to the phase formed on the aluminum side. The EDS analysis on the copper side (P2) also supports this assumption since the Cu-based solid solution Cu(Al) is not observed. When the

concentration of copper atoms at the aluminum side exceeds $C^{\alpha L}$ at the contact points, these regions begin to melt, leading to the formation of the liquid (L). Both copper and aluminum atoms continuously diffuse into L, and the diffusion is controlled by the diffusion coefficient (D_L) in the liquid at this stage. The liquid spreads along the interface, leading to the extrusion of shreds of the oxide films as well as the elimination of voids. The liquid at the interface gradually reaches a chemical composition between $C^{L\alpha}$ and $C^{L\theta}$ ($C^{L\alpha}$ and $C^{L\theta}$ are the chemical compositions of the liquid adjacent to aluminum and copper, respectively). In fact, the composition of the liquid is very close to the eutectic composition of the Cu–Al alloy; hence, the eutectic phase is expected to form during the cooling process. Through isothermal heating, the surface of aluminum adjacent to the liquid has the chemical composition $C^{\alpha L}$, while the liquid in contact with that surface has the chemical composition $C^{L\alpha}$. Simultaneously, the liquid adjacent to the copper has the chemical composition $C^{L\theta}$. From this moment on, the solid embryos of $CuAl_2$ (θ) nucleate. These nuclei have chemical compositions of $C^{\theta L}$ ($C^{\theta L}$ is the chemical composition of the surface of copper adjacent to the liquid) and subsequently enter into the growing step. The morphology appears to be scallop-shaped, and Fig. 7 shows an illustration of the growth of the $CuAl_2$ phase. In Fig. 7, the arrows represent the Cu flux. In general, three paths dominate the growth of $CuAl_2$: (1) the rate of Cu atomic diffusion from the Cu substrate to the $CuAl_2$/L interface; (2) the rate of Al atomic diffusion from L to the $CuAl_2$/L interface; and (3) the rate of Cu atomic diffusion from the peak of a $CuAl_2$ scallop to the valley. Paths 1 and 2 are driven by the Cu and Al atomic concentration gradients, which govern the longitudinal growth of $CuAl_2$; path 3 is driven by the curvature effect, which determines the cross growth of $CuAl_2$ [32]. Nevertheless, the α-Al phase formed on the aluminum side is not distinguished due to its similar structure and color to those of the base metal.

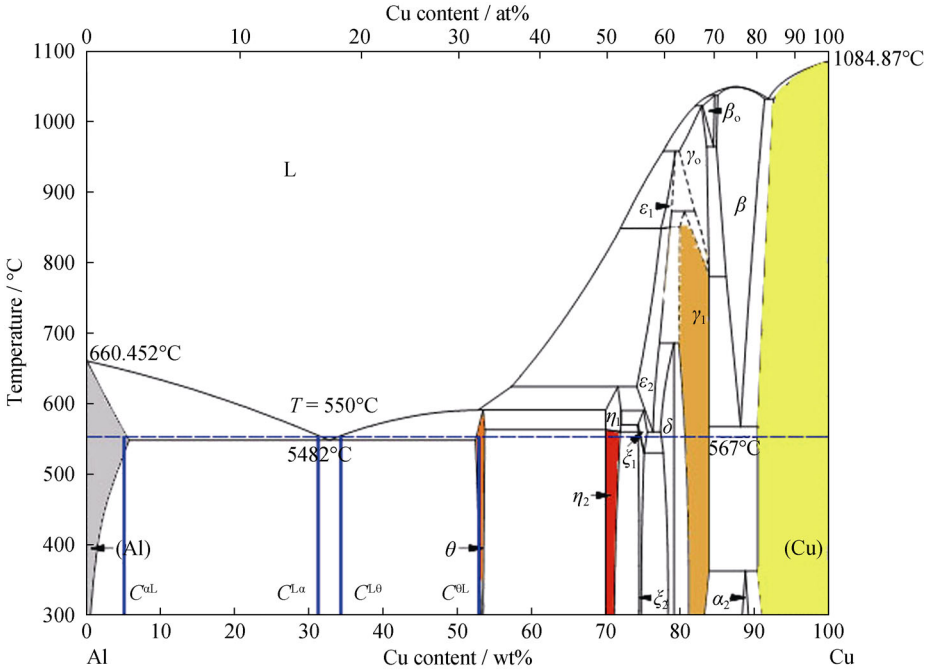

Fig. 6. Cu–Al phase diagram.

As mentioned in Section 3.2.2, the Cu_9Al_4 layer exhibits a planar morphology, while CuAl is discontinuous. Although the experimental results in this study provide no direct evidence of the sequence of phase formation between Cu_9Al_4 and CuAl, the Cu_9Al_4 layer is presumed to form before the CuAl phase based on the relatively large amount of Cu_9Al_4. This assumption is supported by the results of a previous study [33]. In addition, the effective heat of formation model explains that the preferential formation of Cu_9Al_4 over CuAl can be attributed to the higher driving force for formation [7]. The Cu_9Al_4 phase is considered to result from solid-state phase transformation [18]. After the nucleation of $CuAl_2$, the aluminum atoms continue to diffuse from the liquid to the Cu substrate through the solidified $CuAl_2$ phase. During the consumption of the Cu matrix and the $CuAl_2$ phase, $CuAl_2$ reacts with Cu to yield Cu_9Al_4 through solid-state diffusion. As diffusion progresses, $CuAl_2$ and Cu_9Al_4 layers continue to grow until the holding time ends. When the bonding temperature drops, the liquid conventionally transforms to the eutectic structure (α-Al+$CuAl_2$),

and CuAl is generated at the interface of $CuAl_2/Cu_9Al_4$. From the copper side to the aluminum side, the final structure consists of Cu_9Al_4, CuAl, $CuAl_2$, and α-Al+$CuAl_2$.

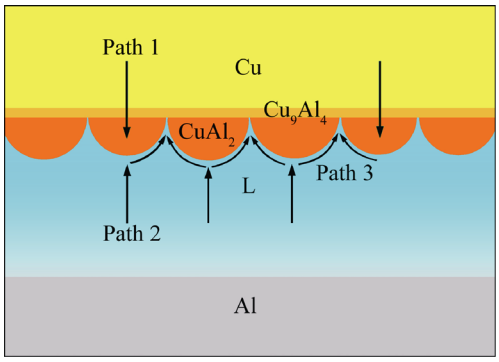

Fig. 7. Schematic of Cu diffusion paths during isothermal heating.

The schematic of the mechanism of the interfacial reaction between Cu and Al is shown in Fig. 8. (1) Due to the application of uniaxial pressure, oxide films rupture at contact points, which is available for interdiffusion between copper and aluminum. (2) When the copper concentration at the aluminum side exceeds $C^{\alpha L}$, the liquid (L) forms in the real contact area and spreads along the interface, thus squeezing out most shreds of the oxide films. (3) With time increasing, the liquid thickens due to the continuous diffusion of both atoms into the liquid, and $CuAl_2$ then nucleates at the Cu/L interface during isothermal heating. (4) After $CuAl_2$ solidifies, Cu_9Al_4 is generated through solid-state phase transformation at the expense of the Cu matrix and $CuAl_2$. (5) The liquid transforms into the eutectic structure when the temperature decreases to ambient temperature; the CuAl phase is presumed to form simultaneously.

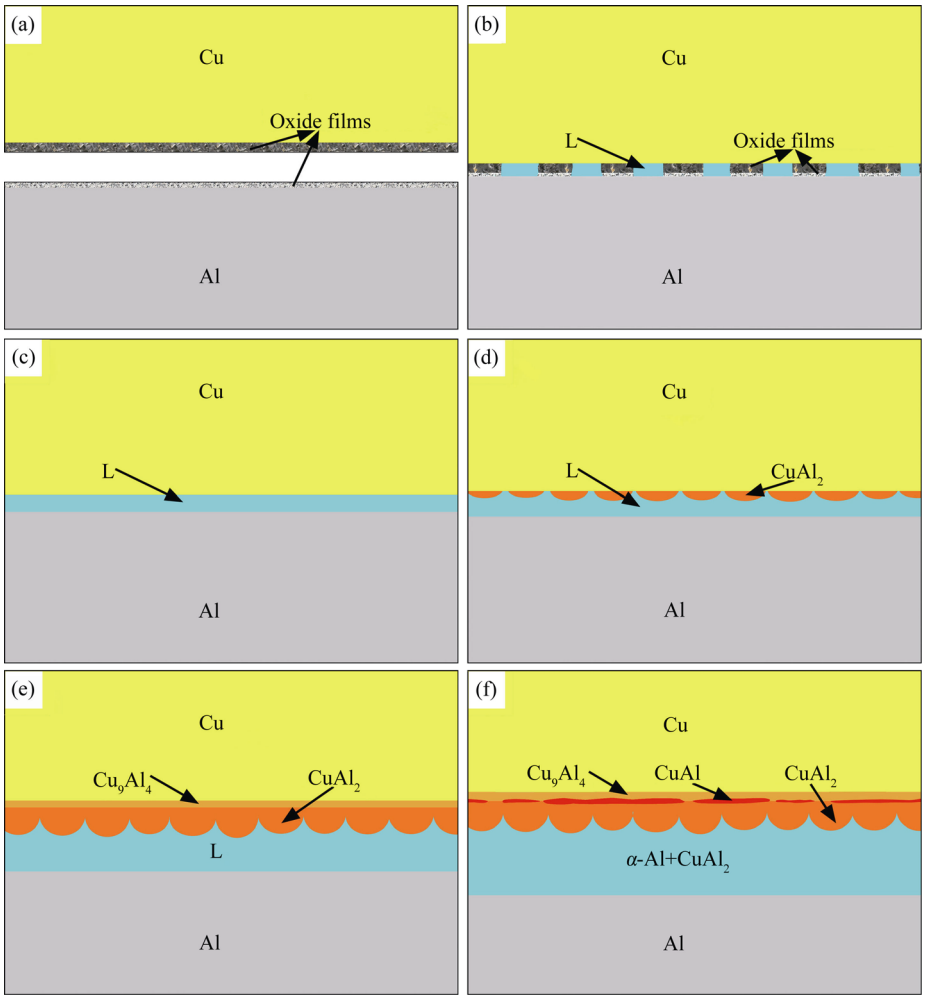

Fig. 8. Schematics of interfacial evolution during isothermal heating: (a) native oxide films on aluminum and copper prior to bonding; (b) liquid is formed at some points; (c) liquid spreads along the interface, and most fragments of oxide films are extruded; (d) $CuAl_2$ is produced during bonding; (e) $CuAl_2$ keeps growing followed by the formation of Cu_9Al_4; (f) CuAl is formed during cooling.

3.5. Hardness of the Cu/Al interface

The Vickers hardness of the interfacial zone shown in Fig. 9 was measured to investigate the effect of chemical composition. It is evident that the hardness is higher at the interface than on the base metals, which most likely results from the compositional change of the interfacial zone. A greater hardness of IMCs signifies very low mechanical integrity, thus leading to the brittleness of the Cu/Al couples [34]. The observed hardness value first increases and peaks at point 1 located at the IMCs/base material interface. It should be noted that the three intermetallic phases (Cu_9Al_4, CuAl, and $CuAl_2$) that cannot be well separated under optical microscopy show a composite hardness of 235 HV. With regard to the eutectic zone, fluctuation in hardness is clearly observed. This can be attributed either to the change in dendritic spacings or to the structural difference between the anomalous region and the lamellar eutectic region. The hardness value of point 2 is slightly higher than that of the base metal owing to the strengthening of the solid solution.

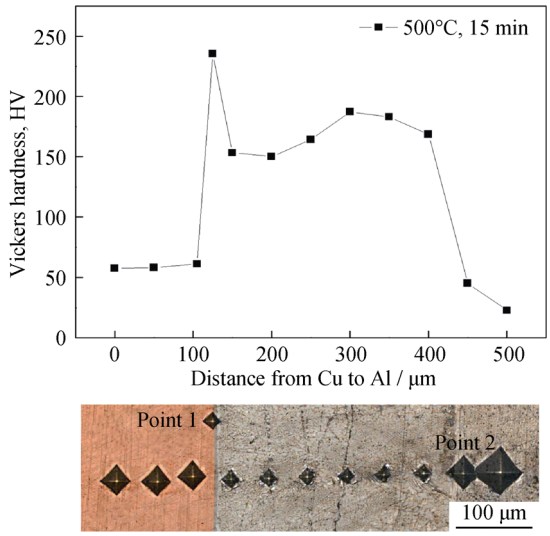

Fig. 9. Vickers hardness profiles across the interfacial zone of the sample bonded at 550°C for 15 min.

4. Conclusions

In this study, the evolutionary process of Cu/Al couples and their mechanism of formation are identified and discussed. In addition, the relationship between chemical composition and mechanical properties is investigated. The following conclusions are made:

(1) Time is required for metallurgical bonding since both Cu and Al atoms are thermally activated and the breakage of oxide films is necessary for interdiffusion and interfacial reaction. Increasing the bonding time from 15 to 25 min results in an increase in reactive zone thickness from 1227 μm to 1423 μm.

(2) The microstructural analysis indicates that the interfacial zone consists of Cu_9Al_4, CuAl, $CuAl_2$, and α-Al+$CuAl_2$ from Cu to Al. The eutectic structure is dominant in the interfacial zone.

(3) The evolutionary process proceeds as follows. Initially, the oxide films rupture followed by the production of the liquid. With increasing time, the movement of the solid/liquid interface attempts to maintain a balance between $C^{L\alpha}$ of the liquid and $C^{\alpha L}$ of the solid on the Al side as well as between $C^{L\theta}$ of the liquid and $C^{\theta L}$ of the solid on the Cu side, resulting in the formation of α-Al and $CuAl_2$. Cu_9Al_4 develops a planar morphology through solid state phase transformation, and both the eutectic structure and CuAl are formed in the cooling process.

(4) The hardness values of intermetallic compounds are higher than those of aluminum or copper base metals. The peak value of the mixture of three intermetallic phases is attributed to their brittle nature.

Acknowledgements

This research was financially supported by the National Natural Science Foundation of China (No. 51274038).

References

[1] Y.J. Guo, G.J. Qiao, W.Z. Jian, and X.H. Zhi, Microstructure and tensile behavior of Cu–Al multi-layered composites prepared by plasma activated sintering, *Mater. Sci. Eng. A*, 527(2010), No. 20, p. 5234.

[2] M. Abbasi, A.K. Taheri, and M.T. Salehi, Growth rate of intermetallic compounds in Al/Cu bimetal produced by cold roll welding process, *J. Alloys Compd.*, 319(2001), No. 1-2, p. 233.

[3] C.Y. Chen and W.S. Hwang, Effect of annealing on the interfacial structure of aluminum–copper joints, *Mater. Trans.*, 48(2007), No. 7, p. 1938.

[4] G. Heness, R. Wuhrer, and W.Y. Yeung, Interfacial strength development of roll-bonded aluminium/copper metal laminates, *Mater. Sci. Eng. A*, 483-484(2008), p. 740.

[5] X.B. Li, G.Y. Zu, M.M. Ding, Y.L. Mu, and P. Wang, Interfacial microstructure and mechanical properties of Cu/Al clad sheet fabricated by asymmetrical roll bonding and annealing, *Mater. Sci. Eng. A*, 529(2011), p. 485.

[6] Y. Funamizu and K. Watanabe, Interdiffusion in Al–Cu system, *Trans. Jpn. Inst. Met.*, 12(1971), No. 3, p. 147.

[7] Y.J. Guo, G.W. Liu, H.Y. Jin, Z.Q. Shi, and G.J. Qiao, Intermetallic phase formation in diffusion-bonded Cu/Al laminates, *J. Mater. Sci.*, 46(2011), No. 8, p. 2467.

[8] C.Y. Chen, H.L. Chen, and W.S. Hwang, Influence of interfacial structure development on the fracture mechanism and bond strength of aluminum/copper bimetal plate, *Mater. Trans.*, 47(2006), No. 4, p. 1232.

[9] W.B. Lee, K.S. Bang, and S.B. Jung, Effects of intermetallic compound on the electrical and mechanical properties of friction welded Cu/Al bimetallic joints during annealing, *J. Alloys Compd.*, 390(2005), No. 1-2, p. 212.

[10] K. Meguro, M.O, and M. Kajihara, Growth behavior of compounds due to solid-state reactive diffusion between Cu and Al, *J. Mater. Sci.*, 47(2012), No. 12, p. 4955.

[11] H. Kawakami, J. Suzuki, and J. Nakajima, Bonding process of Al/Cu dissimilar bonding with liquefaction in air, *Weld. Int.*, 21(2007), No. 12, p. 836.

[12] M. Divandari and J. Campbell, A new technique for the study of aluminum oxide films, *Alum. Trans.*, 2(2000), No. 2, p. 233.

[13] G.F. Zhang, J.X. Zhang, Y. Pei, S.Y. Li, and D.L. Chai, Joining of Al_2O_3p/Al composites by transient liquid phase (TLP) bonding and a novel process of active-transient liquid phase (A-TLP) bonding, *Mater. Sci. Eng. A*, 488(2008), No. 1-2, p. 146.

[14] X.Y. Gu, D.Q. Sun, L. Liu, and Z.Z. Duan, Microstructure and mechanical properties of transient liquid phase bonded TiC_P/AZ91D joints using copper interlayer, *J. Alloys Compd.*, 476(2009), No. 1-2, p. 492.

[15] Y.Y. Qian, Z.G. Dong, and F. Gao, Microstructure development and metallurgical analysis of the Al–Si contact reaction, *J. Mater. Process. Technol.*, 122(2002), No. 2-3, p. 305.

[16] F.A. Calvo, A. Ureng, J.M. Gomez De Salazar, and F. Molleda, Special features of the formation of the diffusion bonded joints between copper and aluminium, *J. Mater. Sci.*, 23(1988), No. 6, p. 2273.

[17] G.Q. Wu, Z.F. Li, G.X. Luo, H.Y. Li, and Z. Huang, Dynamic simulation of solid-state diffusion bonding, *Mater. Sci. Eng. A*, 452-453(2007), p. 529.

[18] Y.J. Su, X.H. Liu, H.Y. Huang, X.F. Liu, and J.X. Xie, Interfacial microstructure and bonding strength of copper cladding aluminum rods fabricated by horizontal core-filling continuous casting, *Metall. Mater. Trans. A*, 42(2011), No. 13, p. 4088.

[19] P. Xue, B.L. Xiao, D.R. Ni, and Z.Y. Ma, Enhanced mechanical properties of friction stir welded dissimilar Al–Cu joint by intermetallic compounds, *Mater. Sci. Eng. A*, 527(2010), No. 21-22, p. 5723.

[20] C.W. Tan, Z.G. Jiang, L.Q. Li, Y.B. Chen, and X.Y. Chen, Microstructural evolution and mechanical properties of dissimilar Al–Cu joints produced by friction stir welding, *Mater. Des.*, 51(2013), p. 466.

[21] H. Xu, C. Liu, V.V. Silberschmidt, S.S. Pramana, T.J. White, Z. Chen, and V.L. Acoff, Behavior of aluminum oxide, intermetallics and voids in Cu–Al wire bonds, *Acta Mater.*, 59(2011), No. 14, p. 5661.

[22] G.R. Zare, M. Divandari, and H. Arabi, Investigation on interface of Al/Cu couples in compound casting, *Mater. Sci. Technol.*, 29(2013), No. 2, p. 190.

[23] J.A. Warren, T. Pusztai, L. Környei, and L. Gránásy, Phase field approach to heterogeneous crystal nucleation in alloys, *Phys. Rev. B*, 79(2009), p. 4204.

[24] D. Moreno, J. Garrett, and J.D. Embury, A technique for rapid characterization of intermetallics and interfaces, *Intermetallics*, 7(1999), No. 9, p. 1001.

[25] J.F. Li, P.A. Agyakwa, and C.M. Johnson, Interfacial reaction in Cu/Sn/Cu system during the transient liquid phase soldering process, *Acta Mater.*, 59(2011), No. 3, p. 1198.

[26] M.S. Park, S.L. Gibbons, and R. Arróyave, Phase-field simulations of intermetallic compound growth in Cu/Sn/Cu sandwich structure under transient liquid phase bonding conditions, *Acta Mater.*, 60(2012), No. 18, p. 6278.

[27] M. Aravind, P. Yu, M.Y. Yau, and Dickon H.L. Ng, Formation of Al_2Cu and AlCu intermetallics in Al(Cu) alloy matrix composites by reaction sintering, *Mater. Sci. Eng. A*, 380(2004), No. 1-2, p. 384.

[28] M. Eizadjou, A.K. Talachi, H.D. Manesh, H.S. Shahabi, and K. Janghorban, Investigation of structure and mechanical properties of multi-layered Al/Cu composite produced by accumulative roll bonding (ARB) process, *Compos. Sci. Technol.*, 68(2008), No. 9, p. 2003.

[29] G.H. Min, J.M. Lee, S.B. Kang, and H.W. Kim, Evolution of microstructure for multilayered Al/Ni composites by accumulative roll bonding process, *Mater. Lett.*, 60(2006), No. 27, p. 3255.

[30] K.J.M. Papis, B. Hallstedt, J.F. Löffler, and P.J. Uggowitzer, Interface formation in aluminium–aluminium compound casting, *Acta Mater.*, 56(2008), No. 13, p. 3036.

[31] E. Hug and N. Bellido, Brittleness study of intermetallic (Cu, Al) layers in copper-clad aluminium thin wires, *Mater. Sci. Eng. A*, 528(2011), No. 22-23, p. 7103.

[32] F. Ji and S.B. Xue, Growth behaviors of intermetallic compound layers in Cu/Al joints brazed with Zn–22Al and Zn–22Al–0.05Ce filler metals, *Mater. Des.*, 51(2013), p. 907.

[33] C.C. Hsieh, M.S. Shi, and W. Wu, Growth of intermetallic phases in Al/Cu composites at various annealing temperatures during the ARB process, *Met. Mater. Int.*, 18(2012), No. 1, p. 1.

[34] M. Braunovic and N. Alexandrov, Intermetallic compounds at aluminum-to-copper electrical interfaces: effect of temperature and electric current, *IEEE Trans. Compon. Packag. Manuf. Technol. Part A*, 17(1994), No. 1, p. 78.